Journal of Nuclear Materials 539 (2020) 152296

Contents lists available at ScienceDirect

Journal of Nuclear Materials

journal homepage: www.elsevier.com/locate/jnucmat

Modeling high burnup structure in oxide fuels for application to fuel performance codes. part I: High burnup structure formation

T. Barani [a, b], D. Pizzocri [a], F. Cappia [c], L. Luzzi [a], G. Pastore [c], P. Van Uffelen [b, *]

[a] Politecnico di Milano, Department of Energy, Nuclear Engineering Division, Via La Masa 34, I-20156, Milano, Italy
[b] European Commission, Joint Research Centre, Directorate for Nuclear Safety and Security, P.O. Box 2340, 76125, Karlsruhe, Germany
[c] Idaho National Laboratory, P.O. Box 1625, Idaho Falls, ID, 83415-3840, United States

ARTICLE INFO

Article history:
Received 18 March 2020
Received in revised form
12 May 2020
Accepted 3 June 2020
Available online 30 June 2020

Keywords:
High burnup structure
Intra-granular fission gas behavior
Oxide fuel
Xenon depletion
Fuel performance codes

ABSTRACT

We propose a model describing the HBS formation and the progressive intra-granular xenon depletion in UO2. The HBS formation is modeled employing the Kolmogorov-Johnson-Mehl-Avrami (KJMA) formalism for phase transformations, which has been fitted to experimental data on the restructured volumetric fraction as a function of the local effective burnup. To this end, we employed available experimental data and novel data extracted in this work. The HBS formation model is coupled to a description of the intra-granular fission gas behavior, allowing to estimate the evolution of the retained xenon in order to consistently compute fission gas retention and its effect on the fuel matrix swelling. The satisfactory agreement of the model predictions to experimental data and state-of-the-art models' results, in terms of both xenon depletion and fuel matrix swelling as a function of the local burnup, paves the way to the inclusion of the model in fuel performance codes.

1. Introduction

In nuclear fuels, where substantial irradiation damage (e.g., local burnups above 45/50 MWd kgU^{-1}) is accompanied by a limited possibility of recovering the damage (i.e., local temperatures below 1000 °C), a dramatic change occurs to the as-fabricated microstructure. The initial microstructure, usually featured by micrometric grain sizes, is gradually replaced by the appearance of submicrometric, re-crystallized grains alongside micrometric pores, of roughly spherical shape. This phenomenon is referred to as High Burnup Structure (HBS), or rim effect, since it was historically observed and postulated to be limited to the restructuring observed in the outer region of Light Water Reactor (LWR) fuel pellets [1–5]. Indeed, this phenomenon has been observed in fuel types other than UO2, e.g., in Pu-rich islands of heterogeneous U–Pu mixed oxides (MOX) fuel [3,6–8], in the rim zone of Fast Breeder Reactor (FBR) U–Pu oxide [9,10], in U–Pu carbides [11], and in U–Mo fuels [12].

Despite intensive experimental and modeling activities for decades, the formation mechanisms of HBS are still debated [3,4,13–15]. HBS formation is ascribed either to a re-crystallization [16–23] or a polygonization [24–29] process.[1] Indeed, commonly observed features encompass the build-up of dislocations [20], the depletion of intra-granular fission gas [3,7,30], the formation of pristine, sub-micrometric grains [26], and development of a novel porosity [31,32].

The (economically) appealing interest in increasing the target burnup of LWR rods constitutes a strong driving force in developing models describing HBS behavior to be included in fuel performance codes (FPC). In facts, the development of HBS porosity brings about an additional fuel swelling source, which must be properly represented to predict UO_2 thermo-mechanical performance at high burnups [15,33]. Moreover, HBS development contributes to determine both fuel thermal conductivity [34] and elastic modulus [35]. Finally, the fission gas stored in HBS porosity plays a major role in determining fission gas release (FGR) and fuel fragmentation (and consequent relocation) during Loss of Coolant Accident (LOCA) [36–39] and Reactivity Initiated Accident (RIA) [40] conditions.

Several models, either semi-empirical or mechanistic, have been

[1] Re-crystallization entails the formation of sub-grains localized in re-crystallization nuclei in the original grains, and the subsequent growth of re-crystallized sub-grains. On the contrary, the polygonization process is the subdivision of original grains, due to the formation of dislocation cells and subsequent birth of new boundary domains into the original grain volume.

* Corresponding author.
E-mail address: paul.van-uffelen@ec.europa.eu (P. Van Uffelen).

https://doi.org/10.1016/j.jnucmat.2020.152296

conceived to describe HBS effects in the framework of FPCs. Since this work is focused on modeling HBS formation and intra-granular fission gas depletion – leaving the description of porosity development to a forthcoming, second part – we limit our discussion to the modeling of these two aspects.

Lassmann et al. [41] developed a pragmatic, empirical model to account for intra-granular xenon depletion, decreasing its concentration with an exponential law as a function of burnup (not considering the effect of temperature) and needing as an input parameter the HBS formation threshold. This approach represents the legacy treatment of HBS in the TRANSURANUS FPC code [42]. In a recent work, Jernkvist [43] adopted the same concept to describe xenon depletion, while combining it to a threshold value estimated by the theoretical model of Rest [44]. The model has been made available to the FRAPCON/FRAPTRAN codes [45]. Lemes et al. [46] extended the model by Lassmann, including the treatment of Kr and complementing it with a mixed empirical and mechanistic description of the porosity development. The model is implemented in the DIONISIO code [47].

The model by Khvostov and coworkers [48,49] describes the HBS restructuring through a Kolmogorov-Johnson-Mehl-Avrami (KJMA) relationship, introducing also the concept of "effective burnup" in the description of HBS to weight differently the burnup accumulation at high and low temperatures and thus consider thermal annealing of defects in the description of HBS formation. The semi-empirical description of HBS formation is then paired to a mechanistic description of intra- and inter-granular gas behavior, grafted in the GRSW-A model [49] and integrated in the FALCON code [50]. The concept of effective burnup was integrated into the Lassmann model by Holt et al. [51], introducing a higher temperature threshold in the definition of effective burnup with respect to the one originally proposed by Khvostov. This model is the standard treatment of the HBS formation/depletion in TRANSURANUS.

Blair and coworkers [52] developed a steady-state model describing the xenon depletion in HBS grains, considering in a physically based manner the main intra-granular behavior processes and focusing on the effects of grain boundary diffusivity and re-solution. The main limits of the model are the lack of description of HBS formation and the steady-state formulation, which prevents its application to transient conditions.

L. Noirot proposed a model accounting for HBS formation based on an empirical estimation of the dislocation density evolution [53]. In this model, the evolving dislocation density is fitted to the data by Nogita and Une [54]. The size-distribution of dislocation density is assumed to be a square pulse, and two thresholds of dislocation densities are employed to estimate the fraction of HBS restructuring. The description is plugged in the MARGARET code, which provides a mechanistic description of fission gas behavior, and is integrated into the ALCYONE code [55,56].

Pizzocri et al. [57] proposed a semi-empirical model describing HBS formation and xenon depletion, representing HBS development as a progressive shrinkage of the average grain size of fuel from the original micrometric to the sub-micrometric size as a function of the local effective burnup. Xenon depletion is reproduced solving an intra-granular diffusion problem featured by a decreasing domain size, resulting in an accelerated diffusion towards the grain boundaries. The model is available in the SCIANTIX code [58].

Besides the aforementioned empirical and semi-empirical models, more mechanistic models have been developed to describe HBS formation. Rest [44] proposed a mechanistic model considering the evolution of cellular dislocation networks as recrystallization nuclei and their interaction with intra-granular bubbles. Based on thermodynamics considerations, i.e., comparing the free energies of the original and re-structured phases, he derived a threshold for HBS formation as a function of the local fission density. It must be noticed that the proposed model cannot account for the observed restructuring starting from the grain boundaries and accompanied by the formation of high-angle grain boundary grains [59]. Veshchunov and Shestak [60] proposed a model accounting for the evolution of point, line, and volume defects under irradiation. The key parameter determining HBS formation is the predicted dislocation density, which is compared to a threshold inferred from experimental data [54] to establish HBS formation. Albeit featuring a consistent description of defects evolution, the transition from original to restructured microstructure is step-wise, thus likely failing to properly describe the gradual xenon depletion experimentally observed. The model is available in the MFPR code [61].Whereas the previous models deal mostly with UO_2, combining the predictions by ALCYONE and image analysis techniques, Bouloré et al. [8] developed a probabilistic model to estimate HBS formation in MIMAS (MIcronized MASterblend) MOX fuel for LWRs, based on xenon EPMA measurements. This model allows one to estimate the portion of restructured fuel at a certain burnup, as well as the retention of fission products in the HBS region. This work is a unique example in the open literature of application of HBS modeling in MIMAS MOX fuel.

In this work, we propose a novel model describing HBS formation, accounting for the progressive Xe depletion and its feedback on the fuel matrix swelling. The HBS formation – i.e., the increase of fuel volume that underwent restructuring as a function of the local effective burnup – is described through the KJMA formalism for phase transitions [62,63]. We derived the coefficients of the KJMA expression fitting the functional form to experimental data on the restructured volume fraction as a function of the local effective burnup. The data employed are a combination of available data in the literature [64] and novel data on UO_2 that we extracted through image analysis and fuel performance simulations of recently published experimental results [59]. The HBS formation is paired to a mechanistic model describing intra-granular fission gas behavior in UO_2 published by some of the present coauthors [65], providing the evolution under irradiation of the intra-granular bubble population, accounting for bubble nucleation, gas atom trapping into and irradiation-induced re-solution from bubbles, along with diffusion to the grain boundaries. Estimating the evolving concentrations of retained gas into the grain allows us to consistently calculate the fuel matrix swelling, i.e., the swelling due to solid fission products and xenon atoms found in the fuel matrix and in intra-granular bubbles, up to high burnups. The contribution of the swelling from the large HBS pores will be dealt with separately in a future publication. We implemented the model in the SCIANTIX code [58], a stand-alone, open-source, meso-scale computer code developed at Politecnico di Milano, aimed at simulating fission gas behavior in nuclear fuel and conceived for coupling/inclusion in fuel performance codes.

We present the stand-alone validation of model predictions, comparing the predicted xenon intra-granular concentration as a function of local burnup to available Electron Probe Micro Analysis (EPMA) data [3,7,30] and to a number of models available in the open literature and meant for application in FPCs [41,46,57]. Moreover, we showcase the capabilities of the developed modeling approach to account for the experimentally observed modification of fuel matrix swelling as HBS forms. In particular, we compare the results obtained considering the present model to the experimental data by Spino and coauthors [66]. The comparison to more refined and mechanistic models, e.g., the model by Veshchunov and Shestak available in the MFPR code [60], is of sure interest in perspective, but is left as a part of an extensive comparison between SCIANTIX and MFPR codes.

The present work presents an original model for HBS formation

Table 1
Relevant characteristics of the considered fuel rod, taken from Ref. [59].

Characteristic	Value/Material
Cladding material	Zircaloy−4
Cladding outer diameter (mm)	10.77
Cladding inner diameter (mm)	9.25
Pellet-cladding gap (μm)	95
Pellet diameter (mm)	9.06
Pellet height (mm)	6.93
Dish volume (%)	1
^{235}U enrichment (%)	2.9
Active fuel height (mm)	3660
Fuel pin height (mm)	3860
Specimen (radial average) burnup (MWd kgU^{-1})	72
Measured Fission Gas Release (%)	2.1

due to polygonization, which is described in a continuous and smooth manner, consistently accounting for the intra-granular fission gas behavior during the formation process. The consistent description of the kinetics of intra-granular fission gas behavior and fuel gaseous swelling, together with the formulation grounded on a physical basis – for both formation and fission gas depletion – results in a model which founds a wider applicability, in terms of operating conditions and fuel types, than state-of-the-art models available in fuel performance codes. These features are reconciled with the needs of models to be included in fuel performance codes by industries and research, i.e., ensuring an acceptable computational burden and an optimal numerical stability. Finally, the inclusion of the developed model in the SCIANTIX code will make it available as an open-source tool to the interested public.

The outline of the paper is hereafter briefly outlined. In Section 2, we present the extraction of new data on HBS formation, which are exploited in Section 3, where we present the formulation of the model for HBS formation and intra-granular depletion. The comparison to experimental results and available model predictions are presented in Section 4, whereas we draw the conclusions in Section 5.

2. Derivation of data on High Burnup Structure formation

In this Section, we present the extraction of novel data on the progressive formation of HBS based on the experimental results by Gerczak and coauthors [59]. In particular, we are interested in quantifying the restructured portion of fuel volume and correlating it to the local effective burnup. As a complementary and independent data-set, we report the experimental results on HBS-restructured volume fraction available in the open literature, and published by J. Noirot and coauthors [64].

2.1. Simulation of the analyzed fuel sample

The fuel sample considered in Ref. [59] was taken from a commercial fuel rod irradiated in the H.B. Robinson PWR. The mother fuel rod characteristics, listed in Table 1, together with the irradiation history reported in Refs. [59,67] were used to build the input for a TRANSURANUS [42] simulation. The calculated fuel central and outer temperatures for the analyzed specimen are reported in Fig. 1, together with the input linear heat rate, as a function of the specimen average burnup.

The calculations of radial burnup and effective burnup exploits the TUBRNP burnup model of TRANSURANUS[2] [41,68] and are reported in Fig. 2 as a function of the relative pellet radius. The effective burnup is a concept introduced by Khvostov and coauthors [48] to

[2] The version of the code employed in this work is the v1m3j18.

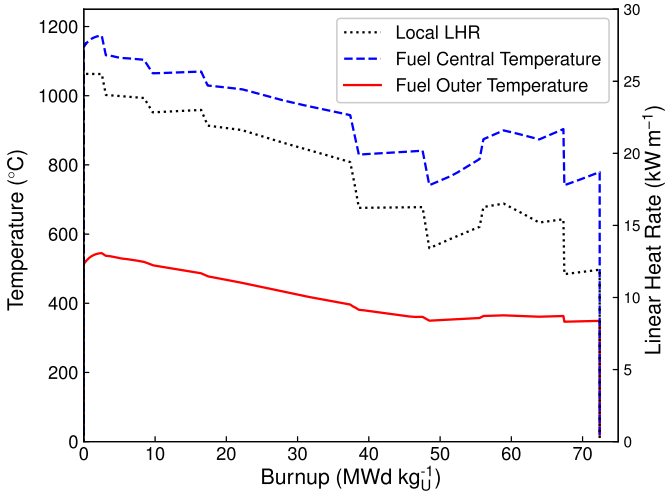

Fig. 1. Linear heat rate and calculated fuel pellet outer and central temperatures as a function of burnup for the considered specimen.

account for the build up of irradiation damage at "low temperatures", i.e., at temperatures at which defects annealing is suppressed. In this work, rather than adopting the original formulation as proposed in Ref. [48], we chose the definition of effective burnup as proposed more recently by Holt and coauthors [51].

$$bu_{eff} = \int f(T-\overline{T})dbu \tag{1}$$

where $f(\overline{T})$ is the Heaviside step function, T (°C) the local temperature, and $\overline{T}$ is a threshold temperature assumed equal to 1000 °C. The estimation of the local (effective) burnup would allow us to complement the information regarding the analyzed experimental data, i.e., associating each analyzed radial position with the corresponding burnup value.

2.2. Extraction of novel data on HBS volume coverage

Gerczak and coworkers [59] investigated the HBS formation

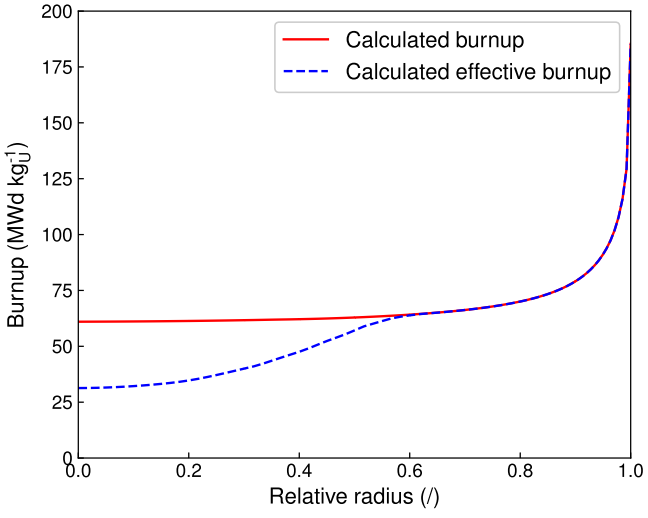

Fig. 2. TRANSURANUS estimation of local and effective burnup as a function of the relative radial position for the considered fuel pellet.

through advanced electron microscopy techniques. In particular, their analysis was focused on the correlation between progressive polygonization and grain boundary surfaces orientations. They showed how low-angle grain boundaries form starting from intra-granular patches and/or from the original high-angle grain boundaries of the as-fabricated microstructure. Moreover, they showed that low-angle grain boundaries are gradually transforming into high-angle grain boundaries moving towards the pellet periphery, i.e., where HBS development is complete. In the aforementioned work, the authors reported Electron Backscatter Diffraction (EBSD) scans of a fuel pellet microstructure, taken at various distances from the pellet outer radius.

In this work, we present the results of further image analysis applied to the aforementioned experimental results, to quantify the HBS surface and volumetric coverage in the examined samples. The image analysis has been performed on the images taken from Figure 10 of the mentioned paper [59], and reported in Fig. 3 for the sake of completeness. We considered a subset of the reported images, focusing on the data obtained at relative radii equal to 0.63, 0.82, 0.94, and 0.95. We assume the image at 0.99 relative radius as representative for the complete restructuring process. This assumption is corroborated by the observed grain size, whose measurement yields approximately 200 nm, roughly corresponding to the observed, asymptotic grain size in the HBS [26,31].

We measured the area covered by HBS in the analyzed locations by the ImageJ software. In particular, we converted to a binary image each analyzed image and quantified the area enclosed by low- and high-angle grain boundaries in the visible sub-domains. The ratio of the selected area to total area of the sample – having discarded the voids and visible porosity – results in the local HBS surface coverage. The results are collected in Table 2, in which we report also an estimation of the volumetric fraction and the estimation of the local effective burnup according to TRANSURANUS predictions.

As for the data presented in the work by J. Noirot et al. [64], the results considered in this work refer to post irradiation examinations of a standard-grain, UO_2 disc irradiated in the Halden Reactor up to an average burnup level of 76 MWd kgU^{-1}. The specifications of the fuel manufacturing, as well as the irradiation conditions are reported in Refs. [64,69]. As the irradiation temperature of the sample is presumed to be below 1000 °C throughout the whole irradiation [64,69], the local burnup estimation is a direct measurement of the effective burnup defined by Eq. (1).

To estimate the burnup as function of the radial position, we employed the information reported in Ref. [64] about the sample irradiation, namely

(i). the average burnup of the sample is equal to 76 MWd kgU^{-1}, and
(ii). the burnup at the periphery of the sample is 19% higher than in the center, to carry out a constrained numerical optimization[3] estimating the burnup at the considered radial positions of the sample. The results of the optimization, in terms of local burnups, together with the experimental data on HBS covered area reported in Ref. [64] and estimated volumetric fractions are reported in Table 3.

3. Formulation of the model for High Burnup Structure formation and fission gas depletion

In this Section, we detail the formulation of the model accounting for HBS formation and intra-granular fission gas behavior. The development of HBS is described through a semi-empirical model, that correlates the fraction of restructured fuel to the local effective burnup. We employed the data derived in Section 2 to derive this model. On the other hand, the behavior of intra-granular fission gas in the restructured volume is described via an available model in the open literature [65]. This model has been tailored to HBS modeling in this work and integrated with the description of HBS restructuring.

3.1. Modeling HBS formation

We employed the data extracted from Refs. [59,64], presented in Section 2, to fit an expression for the HBS formation rate as a function of effective burnup. In particular, we chose the functional form of the Kolmogorov-Johnson-Mehl-Avrami (KJMA) formalism, which is suitable to model generic restructuring phenomena and phase transitions.

The KJMA approach has been already proposed in HBS modeling [48,63], relying on the original formulation by Kolmogorov [62], reading

$$\alpha = 1 - \exp\{-K \cdot t^{\gamma}\} \tag{2}$$

where α (/) is the restructured volume fraction, K ($s^{-\gamma}$) is the transformation rate constant, γ (–) is the so-called Avrami constant, and t (s) the time. It is interesting to notice that a similar expression has been adopted by Bouloré and coworkers [8] to evaluate the HBS restructuring rate in MIMAS uranium-plutonium mixed oxide fuel, based on statistical considerations.

In this work, we preserved the functional form of the KJMA relationship, while we considered the local effective burnup in place of the time and determined the two constants – K and γ – by a least-square fitting of the experimental data presented in Section 2. The fitting procedure yields $K = 2.77 \times 10^{-7}$ and $\gamma = 3.35$ [4] expressing the effective burnup in MWd kgU^{-1}, namely

$$\alpha = 1 - \exp\left\{ -2.77 \times 10^{-7} \cdot \left(bu_{eff}\right)^{3.35} \right\} \tag{3}$$

The experimental data, together with a plot of the resulting correlation, are shown in Fig. 4.

It must be noticed that, although resulting from a fitting procedure, the coefficients we derived for Eq. (2) retain a physical meaning, which is a direct consequence of the KJMA theoretical formulation [70]. In fact, the value of the power to which the burnup variable is taken (i.e., the Avrami constant, γ) can provide information about the nature of the phase transition. A transformation featured by a constant, bulk nucleation rate of the second phase – in the present work, HBS is representing the second phase – and by a bulk growth has a power equal to 4 [70]. On the other hand, if the nucleation sites are preformed, or if transformation happens on grain boundaries in presence of a constant nucleation rate, the power is equal to 3 [70].

In this work, we obtain from the fitting procedure an Avrami constant between 3 and 4. This value reflects a mixed nature of the transformation, i.e., with contributions from bulk nucleation and growth, and from bulk growth from preformed sites combined to a transformation occurring at grain boundaries. In the work by Khvostov and coauthors [48], the Avrami constant was taken equal to 3, i.e., only the latter mechanism was considered. The presence of this mechanism is corroborated by experimental observations and

[3] The method we chose is the Generalized Reduced Gradient method implemented in the Excel solver, using as guess solutions the average burnup.

[4] We carried out a linear fitting taking the natural logarithm of Eq. (2), obtaining a coefficient of determination for the regression (R^2) equal to 0.81.

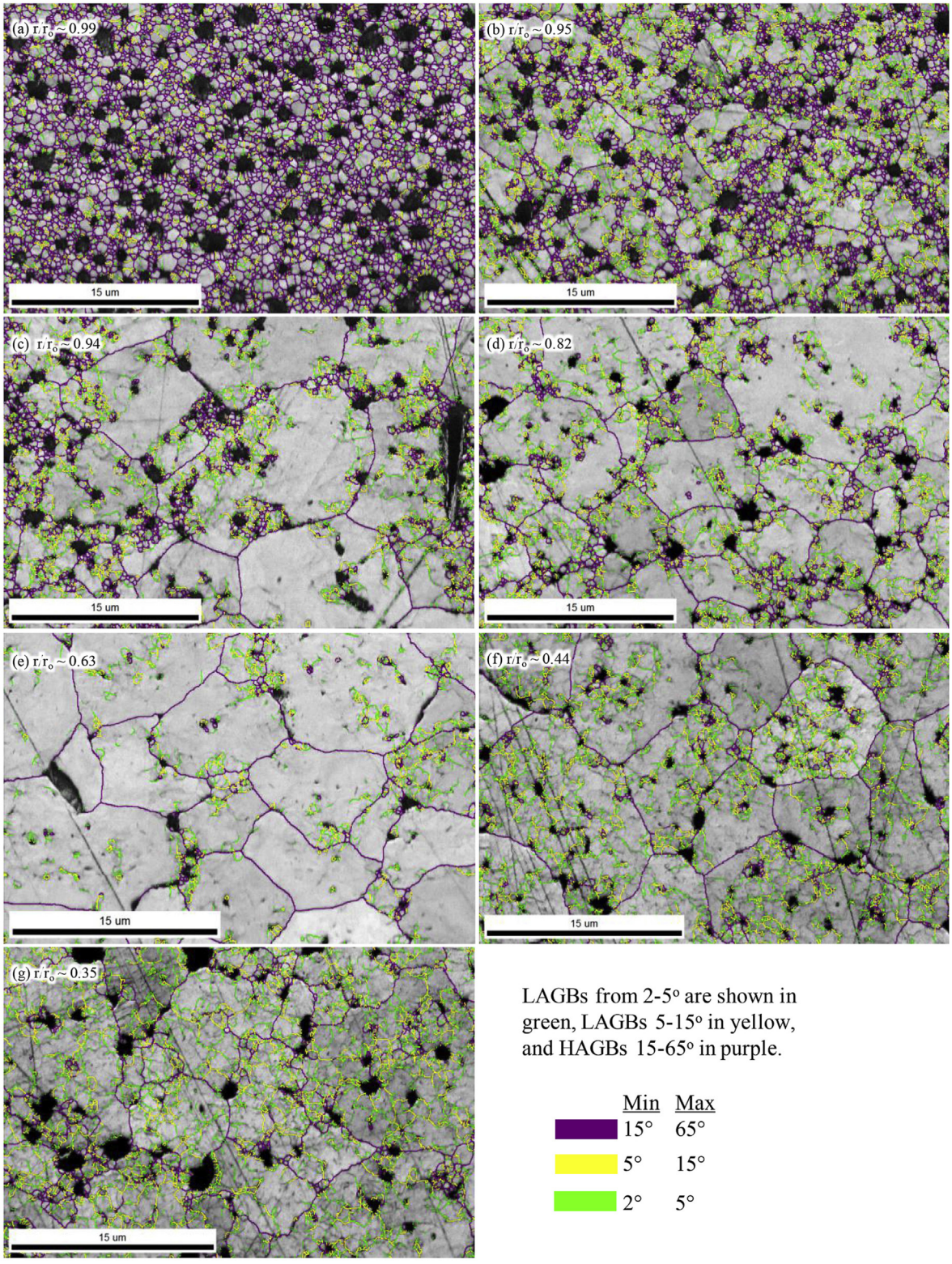

Fig. 3. Grain boundary misorientation map overlaid on image quality map for locations r/r_0 0.99 to 0.35, (a) through (g). Taken from Ref. [59].

theoretical predictions [14,19,31]. This would not account for the formation of HBS following intra-granular patches, which has also been reported in several experimental works [3,14,29,64]. Indeed, the value obtained in this work accounts for all the mentioned contributions, being adherent to the different experimental findings.

For the sake of completeness, we must discuss the validity of the hypotheses underlying the KJMA formalism for phase

Table 2
Measured fraction of re-crystallized area, estimated volumetric fractions and local burnup in the selected locations from the work by Gerczak et al. [59]. The effective and local burnup in the considered radial positions coincide, as shown in Fig. 2.

Relative radius	Effective burnup	HBS-covered area	(Estimated) HBS-covered volume
(/)	(MWd kgU^{-1})	(/)	(/)
0.63	64.7	0.15	0.22
0.82	71.2	0.41	0.54
0.94	88.4	0.54	0.69
0.95	90.8	0.61	0.76
0.99	129.4	1.00	1.00

Table 3
Measured fraction of re-crystallized area, estimated volumetric fractions and local burnup in the selected locations of the sample taken from Ref. [64]. On the basis of the irradiation conditions reported in Refs. [64,69], we postulate that local and effective burnup values coincide.

Relative radial position	Effective burnup	HBS-covered area	(Estimated) HBS-covered volume
(/)	(MWd kgU^{-1})	(/)	(/)
0.30	72.4	0.41	0.55
0.66	77.3	0.46	0.60
0.97	83.8	0.49	0.62

transformation, namely, constant temperature during the transformation, random and homogeneous formation of secondary phase nuclei. The experimental data considered in this work [59], coherently with other recent results [71], corroborate the hypothesis of homogeneous formation of the HBS grains in the original microstructure volume, whereas the random disposition of the nuclei is questionable. In fact, the grain boundaries of the as-fabricated microstructure, as well as the intra-granular fission gas bubbles, appear to be a preferred source for the formation of grain sub-domains. The hypothesis of constant temperature is respected to the extent that in our formulation, the rate of transformation only depends on the effective burnup (Eq. (3)), which in turn is independent of temperature below 1000 °C (Eq. (1)).

3.2. Modeling fission gas depletion in the HBS

As the model is conceived to be included in fuel performance codes, we adopt the classical representation employed in such codes to describe fission gas diffusion, i.e., we represent the single grain as an equivalent spherical domain, employing the concept of an "effective" diffusion equation [15,33,65,72,73].

Equation (3) is adopted to evaluate the volume fraction that underwent HBS restructuring. Besides, the model considers a "two phases" material, one pertaining to the original microstructure and one to HBS, as sketched in Fig. 5.

These two "phases" are featured by different grain sizes, i.e., the original microstructure usually by a micrometric size, whereas the HBS is assumed to be formed at a radius equal to 150 nm (in line with experimental data, e.g., by Ray and coworkers [26]). It is worth to underline that this modeling approach can be naturally extended to heterogeneous U–Pu mixed oxide fuels, featured by "regions" with different Pu content, resulting in local higher fission densities along the fuel pellet.

In both domains, the intra-granular gas behavior is described through the mechanistic model presented by Pizzocri and co-authors [65]. This model allows for the calculation of intra-granular fission gas bubble nucleation, growth due to gas atom trapping, destruction due to the interaction with fission fragments, along with considering a net diffusion of gas atoms towards the grain boundaries. The equations – which are applied in both the original and HBS domains – read

$$\begin{cases} \dfrac{\partial c}{\partial t} = D\nabla^2 c - g_n c + b_n m - 2\nu + y\dot{F} \\ \dfrac{\partial m}{\partial t} = 2\nu + g_n c - b_n m \\ \dfrac{\partial N}{\partial t} = \nu - b_n N \end{cases} \tag{4}$$

where D (m^2 s^{-1}) is the single gas atoms diffusion coefficient, c (at m^{-3}) is the concentration of gas retained in dynamic solution, m (at m^{-3}) is the concentration of gas in the bubbles, N (bubble m^{-3}) is the bubble number density, g_n (s^{-1}) is the trapping rate, b_n (s^{-1}) is the re-solution rate, ν (bubble m^{3}s^{-1}) is the bubble nucleation rate, y (atoms per fission) is the fission gas yield, and $\dot{F}$ (fission m^{3}s^{-1}) is the fission rate density. The average number of atoms in a bubble, n (/), and the associated radius, R (m), and the resulting swelling, $\left(\frac{\Delta V}{V_0}\right)_{ig}$ (/), are defined as

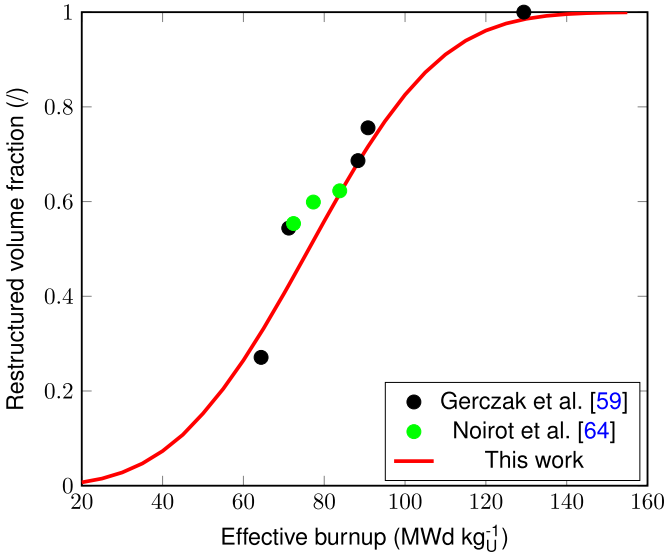

Fig. 4. Experimental measurements derived from Refs. [59,64] on the fraction of restructured fuel volume and KJMA relationship as a function of local effective burnup.

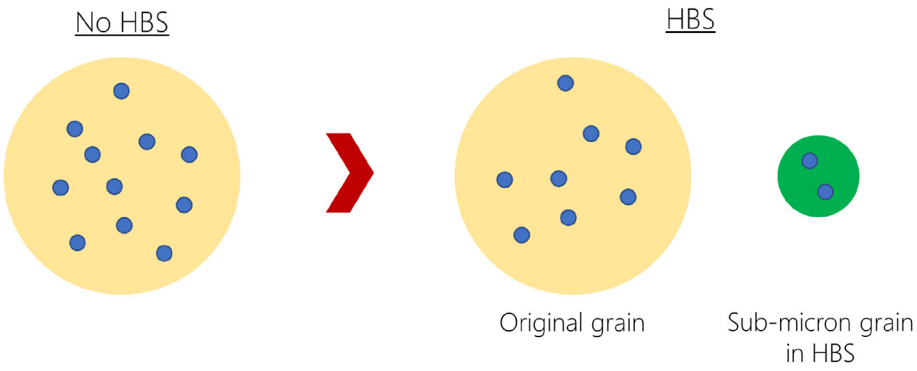

Fig. 5. Representation of the modeling approach to intra-granular fission gas behavior accounting for HBS progressive formation, which introduces a second type of (much smaller) grains.

$$\begin{aligned} n &= \frac{m}{N} \\ R &= Bn^{1/3} \\ \left(\frac{\Delta V}{V_0}\right)_{\text{ig}} &= \frac{4}{3}\pi R^3 N \end{aligned} \tag{5}$$

where $B = (3\Omega/4\pi)^{(1/3)}$ (m) and Ω (m^3) is the volume occupied by a fission gas atom inside intra-granular bubbles in UO_2.

Following Speight [74], we adopt the so-called quasi-stationary approach, i.e., we consider trapping and re-solution to be in equilibrium. Thus, we solve for the total gas concentration in the grain $c_t = c + m$ (at m^{-3}) and simplify Eq. (4) into

$$\begin{cases} \dfrac{\partial c_t}{\partial t} = D_{eff}\nabla^2 c_t + y\dot{F} \\ \dfrac{\partial N}{\partial t} = \nu - b_n N \end{cases} \tag{6}$$

where $D_{eff} = D{\cdot}b/(b+g)$ (m$_2$ s^{-1}) is the "effective" diffusion coefficient. It must be underlined that this approach, i.e., solving a single diffusion equation considering an "effective" diffusion coefficient (Eq. (6)) instead of solving Eq. (4), is the approach currently adopted in state-of-the-art fuel performance codes [15,33] and holds in the majority of normal-operating and accident conditions [75]. However, it presents limitations in modeling rapid transients to relatively high temperatures such as postulated reactivity-initiated accidents (RIA) [75].

As HBS is progressively forming, two intra-granular problems are solved, one for each "phase", considering two different integration domains, characterized by their own grain size (e.g., micrometric in the as-fabricated region and sub-micrometric in the restructured region). Henceforth, the overall concentration of gas in the considered domain,[5] c_t^*, is evaluated as

$$c_t^* = (1-\alpha)\cdot c_t^{NR} + \alpha{\cdot}c_t^{HBS} \tag{7}$$

where the superscripts *NR* and *HBS* refer to the quantities evaluated solving the intra-granular problem in the non-restructured and HBS sub-domains, respectively. The same concept is applied to estimate each concentration. It is worth noticing that this concept of a weighted average is employed also in the MARGARET code [53]. As HBS forms during irradiation, an increasing portion of the material is covered by the restructured microstructure. Thus, we consider a sweeping of gas concentration from the original to restructured region, namely

$$\frac{\partial c_t^{HBS}}{\partial bu_{eff}}\Big|_R = \frac{1}{\alpha}\frac{\mathrm{d}\alpha}{\mathrm{d}bu_{eff}}\left(c_t^{NR} - c_t^{HBS}\right) + \frac{\alpha-1}{\alpha}\frac{\partial c_t^{NR}}{\partial bu_{eff}} \tag{8}$$

where the first term of the right hand side of Eq. (8) represents the effective gas transfer between the two regions due to restructuring. In deriving Eq. (8), we made the assumption of splitting the evolution of the intra-granular gas concentrations accounted by Eq. (6) from the restructuring effects, which are described by Eq. (8).[6] Moreover, we assumed that the total concentration of gas in the considered reference volume is conserved during the restructuring.

The combination of increasing HBS volume ratio and smaller grain size of HBS allows for a consistent description of fission gas depletion as HBS is formed. In facts, as the effective burnup builds up, an increasing fraction of the volume is affected by HBS (Eq. (3)). This increases the weight of intra-granular behavior in the HBS sub-domain, which is characterized by a fast diffusion to the grain boundary associated with the sub-micrometric grain size (the diffusion rate being D/a^2).

Rather than attempting to mechanistically describe HBS formation, whose sequence of phenomena is still debated, the presented approach provides a robust model which accounts for HBS formation and gas depletion in a consistent manner, still preserving a degree of complexity in line with FPCs requirements.

3.3. Modeling fuel matrix swelling

A consistent estimation of fuel matrix swelling, i.e., the swelling due to solid fission product compounds, to fission gas atoms retained in dynamic solution in the matrix, and to the intra-granular fission gas bubbles, must account for the evolution of the gas concentrations as HBS forms as described in Section 3.2.

The total matrix swelling,[7] $\left(\frac{\Delta V}{V_0}\right)_{\text{m}}$ (/), may be expressed as follows

[5] In engineering-scale fuel performance codes, fission gas behavior models are called in each integration point of the fuel computational mesh (e.g., Refs. [33,42,76]).

[6] This treatment is conceptually similar to the treatment of the so-called grain boundary sweeping, i.e., the transfer of gas from the interior of the grains to the grain boundaries due to grain growth (e.g., [77]).

[7] We underline that the swelling due to HBS porosity is not herein considered and will be the subject of a forthcoming second part of this work.

$$\left(\frac{\Delta V}{V_0}\right)_m = \left(\frac{\Delta V}{V_0}\right)_{ig} + \left(\frac{\Delta V}{V_0}\right)_s + \left(\frac{\Delta V}{V_0}\right)_{sg} \quad (9)$$

where the subscript "ig", "s", and "sg" refers to the swelling due to intra-granular bubbles (as defined in Eq. (5)), to the solid fission products, and to the concentration of gas in dynamic solution, respectively. The swelling due to gas in dynamic solution is calculated as

$$\left(\frac{\Delta V}{V_0}\right)_{sg} = c^* \cdot \frac{a^3}{4} \quad (10)$$

where c^* is the overall concentration of gas as single atoms retained in dynamic solution with the matrix (i.e., not in intra-granular bubbles) and a (m) is the UO_2 lattice parameter. In this work, following [78,79], we assume that fission gas atoms are bounded in UO_2 to a Schottky trio (i.e., a neutral complex of defects made of an uranium and two oxygen vacancies). Thus, the associated increment of fuel volume assigned to every gas atom in dynamic solution is three times the average atomic volume in UO_2, equal to $a^3/12$.

As for the swelling due to solid fission products, we rely on the theoretical considerations by Olander [80], who proposed a swelling rate due to fission product compounds not soluble in the UO_2 fluorite structure equal to 0.32% per atom percent burnup. Nonetheless, it must be noticed that solid swelling rate strongly depends on the local chemical speciation, which is governed by the local oxygen potential, whose variation with burnup determines the phases in which elements are found [81]. For example, the previous value obtained by Olander entails considering that all the created Mo is in metallic inclusions, while it is known that as burnup increases Mo can be found as MoO_2 partly dissolved in the fuel matrix [81], determining higher fuel swelling rates (evaluated by Olander as 0.45% per at.%). A more recent and detailed assessment on the basis of various atomic scale calculations (Middleburgh et al. for UO_2 [82], Ducher et al. for UC [83] and Klipfel et al. for UN [84]) accounts for the local environment of each fission product that is also dependent on the evolving stoichiometry. Although we consider a constant value as a function of burnup, in line with state-of-the-art approaches (such as in the MATPRO FSWELL correlation [45]), a shift towards higher values of the swelling rate would be more adherent to the behavior of fission products such as molybdenum. Finally, it must be underlined that state-of-the-art models for fuel matrix swelling do not take into consideration the contribution brought about by irradiation damage, such as the formation of dislocation loops. This contribution is expected to contribute to the swelling rate decreasing associated with HBS formation.

4. Results and discussion

In this Section, we present the results of the presented model, comparing the predictions, in terms of local xenon retention as a function of effective burnup, to available experimental data and to several models available in the open literature and conceived for application to FPCs. Moreover, we showcase the capability of the presented model to account for matrix (macroscopic) swelling modification as HBS formation occurs, due to fission gas atom depletion.

The presented results were obtained implementing the model presented in Section 3 into the SCIANTIX code [58], a stand-alone, meso-scale computer code developed at Politecnico di Milano, aimed at simulating fission gas behavior in nuclear fuels. The expressions of parameters mentioned in Section 3 and employed in SCIANTIX are reported in Table 4.

4.1. Xenon depletion

In Fig. 6, we compare the intra-granular concentration of xenon predicted by SCIANTIX simulations, considering the present model, to several experimental data obtained by different authors [3,7,30] via EPMA. Considering the huge scattering of the experimental data, due to different irradiation conditions and initial fuel specifications, the agreement is deemed satisfactory. For the sake of completeness, it must be underlined that xenon is accompanied by other gases in determining the overall gas behavior (namely, krypton and helium). In this work, we draw a special attention on xenon since it was the subject of the most intensive experimental investigations.

For the sake of comparison, we report also the results obtained by several state-of-the-art models employed in FPCs, namely the model by Lassmann et al. [41], by Lemes et al. [46], and by Pizzocri et al. [57]. The models by Lassmann and Lemes, the latter being an extension of the former, represent pragmatic and purely empirical approaches to account for fission gas depletion as HBS forms, considering an exponential decay of retained gas concentration with burnup. Indeed, they are directly fitted on a subset of the reported EPMA data, i.e., those by Walker [30]. Moreover, they consider a threshold for HBS formation solely dependent on burnup, discarding the effect of temperature, which is instead considered in this work via the effective burnup concept. In Fig. 6, predictions of those models considering different burnup thresholds are reported, showing how this parameter impacts the maximum xenon retention and the subsequent depletion. We underline that in this Figure the burnup and effective burnup coincide, since the data were taken from the rim zone of commercial UO_2 fuel, where the fuel local temperature remains below 1000 °C.

On the other hand, the model proposed by Pizzocri et al. [57] represents a step forward with respect to the aforementioned ones, as it is not purely empirical. This model represents HBS formation by a gradual reduction of the grain size, which may be a questionable representation of the underlying physical processes. Differently from the present model results, the predictions obtained through this model and shown in Fig. 6 are obtained considering a xenon production rate adjusted to the experimental data at low burnups to Walker data [30], to obtain a maximum xenon retention in line with experimental data. Finally, this model does not consider the evolution of intra-granular fission gas bubbles, employing a fixed value for intra-granular bubble density and radius, and disregards volume changes due to irradiation damage in

Table 4
Expressions of the model parameters.

Parameter	Expression/Value	Reference
D^{NR}	$D^{NR} = D_1+D_2+D_3$	[91]
	$D_1 = 7.6 \cdot 10^{-10} \exp\{-4.86 \cdot 10^{-19}/k_B T\}$	
	$D_2 = 5.64 \cdot 10^{-25} \sqrt{\dot{F}} \exp\{-1.91 \cdot 10^{-19}/k_B T\}$	
	$D_3 = 2 \cdot 10^{-40} \cdot \dot{F}$	
	k_B (J K^{-1}), Boltzmann constant	
	T (K), local temperature	
D^{HBS}	$D^{HBS} = 4.5 \cdot 10^{-42} \cdot \dot{F}$	[57,92]
g_n	$g_n = 4\pi DNR(n)$	[93]
b_n	$b_n = 2\pi\mu_{ff}\dot{F}(R(n)+R_{ff})^2$	[94]
	$\mu = 6.0 \cdot 10^{-6} m$, fission fragment track length	[94]
	$R_{ff} = 1.0 \cdot 10^{-9} m$, fission fragment track radius	[94]
ν	$\nu = 2 \cdot 25 \cdot \dot{F}$	[65,73]
Ω	$4.09 \cdot 10^{-29}$ m^3	E.g., [65]
a	$5.47 \cdot 10^{-10}$ m	–

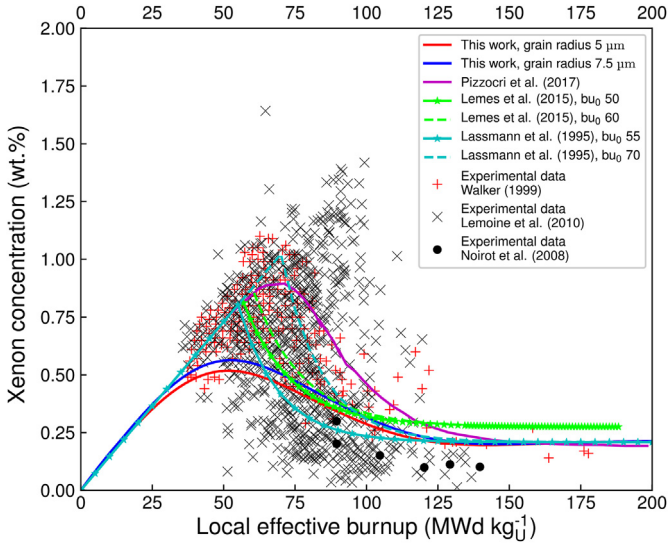

Fig. 6. Comparison of various data on intra-granular xenon concentration obtained via EPMA (red crosses from Walker [30], black crosses from Lemoine et al. [7], and black dots from Noirot et al. [3]) to the predictions of the presented model. For the sake of comparison, the prediction obtained with other state-of-the-art models employed in fuel performance codes are included, namely from Pizzocri et al. [57], Lemes et al. [46], and Lassmann et al. [41]. (For interpretation of the references to colour in this figure legend, the reader is referred to the Web version of this article.)

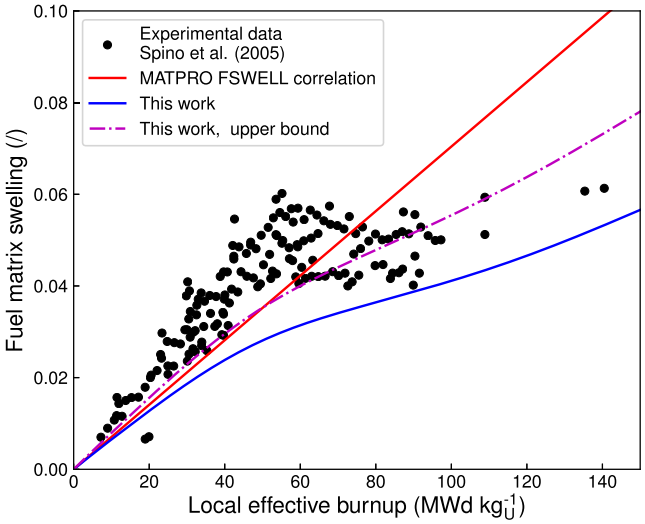

Fig. 7. Comparison of predicted results on matrix fuel swelling to data elaborated by Spino et al. [66], based on Xe retention data obtained through EPMA by Walker [30]. The predictions by the present model – solid blue and dot-dashed purple lines – differ by the considered solid fission product swelling rate, whereas the swelling rate due to intra-granular bubbles and Xenon atom in the matrix is calculated in the same manner. (For interpretation of the references to colour in this figure legend, the reader is referred to the Web version of this article.)

the lattice. This results in an inconsistent estimation of gas partition between bubbles and dynamic solution, preventing a consistent calculation of matrix swelling due to single gas atoms and intra-granular bubbles, in addition to affect the "effective diffusion" representation.

The present model also accounts for the observed delay in xenon depletion (thus HBS formation) when considering higher grain sizes in the original microstructure, as shown in Fig. 6 and coherently with several experimental observations [20,64].

4.2. Fuel total matrix swelling

In Fig. 7, we compare the predictions obtained on the fuel total matrix swelling (as defined in Section 3.3) as a function of effective burnup (as for Fig. 6, also in this case effective and local burnup coincide) to the data compiled by Spino et al. [66]. The matrix swelling predicted by the MATPRO FSWELL model – which is employed in several state-of-the-art fuel performance codes to evaluate the swelling due to solid fission products (e.g., in TRANSURANUS [42], BISON [76], FRAPCON/FRAPTRAN [45]) – is included for comparison and discussion.

The results obtained through the present model, both with the nominal and upper solid fission products swelling rates, demonstrate the impact of the matrix depletion of fission gas as HBS progressively forms. The depletion of fuel matrix, starting predominantly around 60 MWd kgU^{-1}, is likely causing a decrease of the fuel matrix swelling rate,[8] in accordance with the elaboration presented by Spino et al. [66] and based on EPMA results on Xe retention. The agreement of the predicted trend of matrix swelling with the considered data is encouraging. As for the absolute value, the matrix swelling obtained with the nominal swelling rate ascribed to solid fission products (solid blue line in Fig. 7), i.e., 0.32% per atom percent burnup[9] [80], and considering the volume occupied by xenon in dynamic solution and intra-granular bubbles is somewhat underestimating the data reported and the values predicted via the MATPRO FSWELL model. On the other hand, the results obtained considering the upper bound of the solid swelling rate – 0.45% per atom percent burnup [80] – yields a better agreement with the considered data and with the MATPRO FSWELL model.

However, it must be noticed that the interpretation by Spino and coworkers of the data by Walker [30] entails a likely overestimation of the volume occupied by xenon atoms in intra-granular fission gas bubbles. To estimate the swelling due to intra-granular bubbles, the authors assume intra-granular bubbles to be in equilibrium and to obey the van der Waals equation of state [66]. The applicability of both the assumptions is questionable. On one hand, intra-granular bubbles forming under irradiation are far from being in equilibrium [86–88], thus, considering equilibrium bubble, the estimated radii are overestimated. On the other hand, the applicability of van der Waals equation of state to intra-granular bubbles is debatable, due to the high gas densities reached in intra-granular bubbles [86,87]. This calls for the consideration of more advanced equations of state, e.g. the modified hard sphere equation of state proposed by Ronchi [89]. Based on these considerations, we postulate that the data presented by Spino and coauthors in [66] and reported in Fig. 7 may somewhat be an overestimation of the actual portion of fuel matrix swelling ascribed to intra-granular gas.

5. Conclusions

In this work, we presented a novel model describing HBS formation and fission gas depletion in UO_2, conceived for application in fuel performance codes. The model is featuring a semi-empirical,

[8] As discussed in Section 3.3, we speculate that the removal of irradiation damage (i.e., dislocation loops) associated to the formation of pristine HBS grains might contribute to the lower swelling rate observed in this burnup range. We envisage to confirm this postulation and to assess the impact of the chemical speciation on solid product swelling by means of the MFPR-F code [85] in a future work.

[9] The conversion adopted in this work from atom percent burnup to MWd kgU^{-1} is 1 at.% = 9.38 MWd kgU^{-1}.

yet physically sound, description of HBS formation, described through the KJMA approach for phase transformation. We fitted the KJMA functional form to two sets of independent experimental data available in the open literature. In particular, the volume fraction of restructured fuel was correlated to the local effective burnup, i.e., the burnup accumulated below 1000 °C, which was chosen as a lumped figure embodying the effect of irradiation damage and prevented annealing of the damage itself.

The model provides a consistent and continuous description of HBS formation and associated intra-granular fission gas behavior. In facts, the intra-granular fission gas behavior in the re-structured and original microstructure is described through a previously developed mechanistic model. This modeling approach allows us to evaluate the evolution under irradiation of the intra-granular concentration of fission gas in the matrix and trapped into bubbles, together with the estimation of the diffusional flux towards the grain boundaries. The consistent, physically-grounded description of the kinetics of gas behavior and fuel restructuring paves the way to a wide applicability of the model in terms of operating conditions and fuel types, especially if compared to other state-of-the-art models used in industrial fuel performance codes, which constitutes the objective of our modeling effort. In this regard, the present model is compatible with the requirements in terms of numerical stability and computational burden for the inclusion in fuel performance codes, while preserving a certain degree of physical basis on the considered phenomena.

A first comparison of the stand-alone model predictions to experimental data indicates a good agreement in terms of retained intra-granular xenon concentration, also when compared to other semi-empirical models available in the open literature. The model can reproduce the experimentally observed delay in xenon depletion – connected to a delayed HBS formation – when the original microstructure is featured by larger grain sizes. Moreover, the results in terms of matrix fuel swelling predicted by the model are well reproducing the experimentally observed change in fuel matrix swelling rate at high burnup, as a consequence of the depletion of the xenon retained in dynamic solution with the matrix.

The model has been implemented into the SCIANTIX code and will be distributed open-source. The present work represents the first part of a modeling effort devoted to the development of a comprehensive model describing HBS formation in UO_2 and conceived for inclusion in fuel performance codes. Forthcoming works will tackle the evolution of HBS porosity and consequent fuel gaseous swelling, as well as a more extended and integral assessment of the overall model on fuel performance simulations, namely via the TRANSURANUS/SCIANTIX code suite, of high burnup rods.

As future perspective on the presented work, we envisage to enlarge the fitting data-set of the KJMA relation, analyzing other experimental databases (such as the High Burnup Rim Project [90]). Moreover, the developed modeling approach paves the way to the analysis of HBS in other oxide fuel concepts. Indeed, the “two phases” modeling strategy find a natural application to MIMAS MOX fuels, thus an analysis of this type of fuels is of interest in perspective. As for FBR U–Pu oxide, few experimental data are available in the open literature on the HBS in such conditions. The trends would suggest a possible delay in HBS formation as a function of the local burnup and a different asymptotic grain size in the restructured zone, with a consequent lower xenon retention. Indeed, as new data on this side would be available, a tailoring of the current model formulation would be of interest.

CRediT authorship contribution statement

T. Barani: Conceptualization, Methodology, Software, Validation, Writing - original draft, Writing - review & editing, Visualization. **D. Pizzocri:** Conceptualization, Methodology, Software, Writing - review & editing. **F. Cappia:** Conceptualization, Writing - review & editing. **L. Luzzi:** Writing - review & editing, Funding acquisition, Supervision. **G. Pastore:** Writing - review & editing, Supervision. **P. Van Uffelen:** Conceptualization, Methodology, Software, Writing - original draft, Writing - review & editing, Funding acquisition, Supervision.

Declaration of competing interest

The authors declare that they have no known competing financial interests or personal relationships that could have appeared to influence the work reported in this paper.

Acknowledgments

This work has been partially supported by the ENEN + project that has received funding from the Euratom research and training Work Programme 2016–2017–1 #755576, and has received funding from the Euratom research and training programme 2014–2018 through the INSPYRE Project under grant agreement No. 754329.

This work contributes to the Joint Programme on Nuclear Materials (JPNM) of the European Energy Alliance (EERA), in the specific framework of the COMBATFUEL Project, and to the U.S.-EURATOM International Nuclear Energy Research Initiative (INERI) project 2017-004-E on Modelling of Fission Gas Behaviour in Uranium Oxide Nuclear Fuel Applied to Engineering Fuel Performance Codes.

The submitted manuscript has been authored by a contractor of the U.S. Government under Contract DE-AC07-05ID14517. Accordingly, the U.S. Government retains a non-exclusive, royalty free license to publish or reproduce the published form of this contribution, or allow others to do so, for U.S. Government purposes.

References

[1] W. Barney, B. Wemble, Metallography of UO2-Containing Fuel Elements, Tech. Rep. KAPL 1836, 1958.
[2] J. Belle, Uranium Dioxide: Properties and Nuclear Applications, vol. 4, Naval Reactors, Division of Reactor Development, US Atomic Energy Commission, 1961.
[3] J. Noirot, L. Desgranges, J. Lamontagne, Detailed characterisations of high burn-up structures in oxide fuels, J. Nucl. Mater. 372 (2-3) (2008) 318–339.
[4] V.V. Rondinella, T. Wiss, The high burn-up structure in nuclear fuel, Mater. Today 13 (2010) 24–32.
[5] T. Wiss, V.V. Rondinella, R.J.M. Konings, D. Staicu, D. Papaioannou, S. Bremier, P. Pöml, O. Benes, J.-Y. Colle, P. Van Uffelen, A. Schubert, F. Cappia, M. Marchetti, D. Pizzocri, F. Jatuff, W. Goll, T. Sonoda, A. Sasahara, S. Kitajima, M. Kinoshita, Properties of the high burnup structure in nuclear light water reactor fuel, Radiochim. Acta 105 (2017) 893–906.
[6] C.T. Walker, M. Coquerelle, Correlation between microstructure and fission gas release in high burnup UO_2 and MOX fuel, in: Proceedings International Topical Meeting on Light Water Reactor Fuel Performance, Avignon, France vol. 506, 1991.
[7] F. Lemoine, D. Baron, P. Blanpain, Key parameters for the high burnup structure fromation thresholds, in: 2010 LWR Fuel Performance Meeting/Top Fuel/WRFPM, Orlando, Florida, USA, 2010.
[8] A. Bouloré, L. Aufore, E. Federici, P. Blanpain, R. Blachier, Advanced characterization of MIMAS MOX fuel microstructure to quantify the HBS formation, Nucl. Eng. Des. 281 (2015) 79–87.
[9] C.T. Walker, G. Nicolaou, Transmutation of neptunium and americium in a fast neutron flux: EPMA results and KORIGEN predictions for the Superfact fuels, J. Nucl. Mater. 218 (1995) 129–138.
[10] K. Maeda, K. Katsuyama, T. Asaga, Fission gas release in FBR MOX fuel irradiated to high burnup, J. Nucl. Mater. 346 (2-3) (2005) 244–252.
[11] I.L.F. Ray, H.J. Matzke, Observation of a high burnup rim-type structure in an advanced plutonium–uranium carbide fuel, J. Nucl. Mater. 250 (2) (1997) 242–243.
[12] A. Leenaers, W. Van Renterghem, S. Van den Berghe, High burn-up structure of U(Mo) dispersion fuel, J. Nucl. Mater. 476 (2016) 218–230.
[13] H.J. Matzke, M. Kinoshita, Polygonization and high burnup structure in nuclear fuels, J. Nucl. Mater. 247 (1997) 108–115.
[14] D. Baron, M. Kinoshita, P. Thevenin, R. Largenton, Discussion about HBS transformation in high burn-up fuels, Nucl. Eng. Technol. 41 (2) (2009)

199–214.
[15] J. Rest, M. Cooper, J. Spino, J. Turnbull, P. Van Uffelen, C. Walker, Fission gas release from UO_2 nuclear fuel: a review, J. Nucl. Mater. 513 (2019) 310–345.
[16] K. Nogita, K. Une, Radiation-induced microstructural change in high burnup UO_2 fuel pellets, Nucl. Instrum. Methods Phys. Res. Sect. B Beam Interact. Mater. Atoms 91 (1994) 301–306.
[17] J. Rest, G. Hofman, Dynamics of irradiation-induced grain subdivision and swelling in U_3Si_2 and UO_2 fuels, J. Nucl. Mater. 210 (1-2) (1994) 187–202.
[18] M. Kinoshita, Towards the mathematical model of rim structure formation, J. Nucl. Mater. 248 (1997) 185–190.
[19] K. Nogita, K.M. Une Hirai, K. Ito, Effect of grain size on recrystallization in high burnup fuel pellets, J. Nucl. Mater. 248 (1997) 196–203.
[20] K. Nogita, K. Une, M. Hirai, K. Ito, K. Ito, Y. Shirai, Effect of grain size on recrystallization in high burnup fuel pellets, J. Nucl. Mater. 248 (1997) 196–203.
[21] J. Rest, G. Hofman, An alternative explanation for evidence that xenon depletion, pore formation, and grain subdivision begin at different local burnups, J. Nucl. Mater. 277 (2-3) (2000) 231–238.
[22] K. Une, K. Nogita, T. Shiratori, K. Hayashi, Rim structure formation of isothermally irradiated UO_2 fuel discs, J. Nucl. Mater. 288 (1) (2001) 20–28.
[23] H. Xiao, C. Long, H. Chen, Model for evolution of grain size in the rim region of high burnup UO_2 fuel, J. Nucl. Mater. 471 (2016) 74–79.
[24] H.J. Matzke, On the rim effect in high burnup UO_2 LWR fuels, J. Nucl. Mater. 189 (1) (1992) 141–148.
[25] H.J. Matzke, A. Turos, G. Linker, Polygonization of single crystals of the fluorite-type oxide UO_2 due to high dose ion implantation +, Nucl. Instrum. Methods Phys. Res. Sect. B Beam Interact. Mater. Atoms 91 (1) (1994) 294–300.
[26] I.L.F. Ray, H.J. Matzke, H.A. Thiele, M. Kinoshita, An electron microscopy study of the RIM structure of a UO_2 fuel with a high burnup of 7.9% FIMA, J. Nucl. Mater. 245 (2-3) (1997) 115–123.
[27] T. Sonoda, M. Kinoshita, I. Ray, T. Wiss, H. Thiele, D. Pellottiero, V. Rondinella, H. Matzke, Transmission electron microscopy observation on irradiation-induced microstructural evolution in high burn-up UO_2 disk fuel, Nucl. Instrum. Methods Phys. Res. Sect. B Beam Interact. Mater. Atoms 191 (1) (2002) 622–628.
[28] T. Sonoda, M. Kinoshita, N. Ishikawa, M. Sataka, A. Iwase, K. Yasunaga, Clarification of high density electronic excitation effects on the microstructural evolution in UO_2, Nucl. Instrum. Methods Phys. Res. Sect. B Beam Interact. Mater. Atoms 268 (19) (2010) 3277–3281.
[29] M. Chollet, G. Kuri, D. Grolimund, M. Marrtin, L. Bertsch, Synchrotron XRD analysis of irradiated UO_2 fuel at various burn-up, in: TopFuel 2016: LWR Fuels with Enhanced Safety and Performance, Boise, Idaho, USA, 2016.
[30] C. Walker, Assessment of the radial extent and completion of recrystallisation in high burn-up UO_2 nuclear fuel by EPMA, J. Nucl. Mater. 275 (1) (1999) 56–62.
[31] J. Spino, A.D. Stalios, H. Santa Cruz, D. Baron, Stereological evolution of the rim structure in PWR-fuels at prolonged irradiation: dependencies with burn-up and temperature, J. Nucl. Mater. 354 (1-3) (2006) 66–84.
[32] F. Cappia, D. Pizzocri, A. Schubert, P. Van Uffelen, G. Paperini, D. Pellottiero, R. Macian-Juan, V.V. Rondinella, Critical assessment of the pore size distribution in the rim region of high burnup UO_2 fuels, J. Nucl. Mater. 480 (2016) 138–149.
[33] P. Van Uffelen, J. Hales, W. Li, G. Rossiter, R. Williamson, A review of fuel performance modelling, J. Nucl. Mater. 516 (2019) 373–412.
[34] C. Ronchi, M. Sheindlin, D. Staicu, M. Kinoshita, Effect of burn-up on the thermal conductivity of uranium dioxide up to 100.000 MWd t^{-1}, J. Nucl. Mater. 327 (1) (2004) 58–76.
[35] F. Cappia, D. Pizzocri, M. Marchetti, A. Schubert, P.V. Uffelen, L. Luzzi, D. Papaioannou, R. Macián-Juan, V. Rondinella, Microhardness and Young's modulus of high burn-up UO_2 fuel, J. Nucl. Mater. 479 (2016) 447–454.
[36] OECD - NEA, Nuclear Fuel Behaviour in Loss-of-Coolant Accident (LOCA) Conditions, Tech. Rep. NEA 6846, 2009.
[37] J. Noirot, Y. Pontillon, S. Yagnik, J. Turnbull, T. Tverberg, Fission gas release behaviour of a 103 GWd/tHM fuel disc during a 1200°C annealing test, J. Nucl. Mater. 446 (2014) 163–171.
[38] A. Bianco, C. Vitanza, M. Seidl, A. Wensauer, W. Faber, R. Macián-Juan, Experimental investigation on the causes for pellet fragmentation under LOCA conditions, J. Nucl. Mater. 465 (2015) 260–267.
[39] OECD - NEA, Report on Fuel Fragmentation, Relocation, Dispersal, Tech. Rep., 2016. NEA-CSNI-R(2016)16.
[40] OECD - NEA, Nuclear Fuel Behaviour During Reactivity Initiated Accidents, Tech. Rep., 2010. NEA-CSNI-R(2010)7.
[41] K. Lassmann, C. Walker, J. van de Laar, F. Lindström, Modelling the high burnup UO_2 structure in LWR fuel, J. Nucl. Mater. 226 (1995) 1–8.
[42] K. Lassmann, TRANSURANUS: a fuel rod analysis code ready for use, J. Nucl. Mater. 188 (C) (1992) 295–302.
[43] L.O. Jernkvist, Modelling of fine fragmentation and fission gas release of UO_2 fuel in accident conditions, EPJ Nucl. Sci. Technol. 5 (2019) 11.
[44] J. Rest, A model for the influence of microstructure, precipitate pinning and fission gas behavior on irradiation-induced recrystallization of nuclear fuels, J. Nucl. Mater. 326 (2) (2004) 175–184.
[45] K. Geelhood, W. Luscher, P. Raynaud, I. Porter, FRAPCON-4.0: A Computer Code for the Calculation of Steady-state, Thermal-Mechanical Behavior of Oxide Fuel Rods for High Burnup, Tech. Rep., PNNL-19417 1 Rev, 2015, 2.
[46] M. Lemes, A. Soba, A. Denis, An empirical formulation to describe the evolution of the high burnup structure, J. Nucl. Mater. 456 (2015) 174–181.
[47] A. Denis, A. Soba, Simulation of pellet-cladding thermomechanical interaction and fission gas release, Nucl. Eng. Des. 223 (2) (2003) 211–229.
[48] G. Khvostov, V. Novikov, A. Medvedev, S. Bogatyr, Approaches to modeling of high burn-up structure and analysis of its effects on the behaviour of light water reactor fuels in the START-3 fuel performance code, in: Water Reactor Fuel Performance Meeting/WRFPM 2005, 2005.
[49] G. Khvostov, K. Mikityuk, M.A. Zimmermann, A model for fission gas release and gaseous swelling of the uranium dioxide fuel coupled with the FALCON code, Nucl. Eng. Des. 241 (8) (2011) 2983–3007.
[50] Y. Rashid, R. Dunham, R. Montgomery, Fuel analysis and licensing code: FALCON MOD01 volume 1, Theor. Numerical Bases 1 (3) (2004) 246.
[51] L. Holt, A. Schubert, P. Van Uffelen, C.T. Walker, E. Fridman, T. Sonoda, Sensitivity study on Xe depletion in the high burn-up structure of UO_2, J. Nucl. Mater. 452 (1-3) (2014) 166–172.
[52] P. Blair, A. Romano, C. Hellwig, R. Chawla, Calculations on fission gas behaviour in the high burnup structure, J. Nucl. Mater. 350 (3) (2006) 232–239.
[53] L. Noirot, MARGARET: a comprehensive code for the description of fission gas behavior, Nucl. Eng. Des. 241 (6) (2011) 2099–2118.
[54] K. Nogita, K. Une, Irradiation-induced recrystallization in high burnup UO_2 fuel, J. Nucl. Mater. 226 (3) (1995) 302–310.
[55] J. Sercombe, I. Aubrun, C. Nonon, Power ramped cladding stresses and strains in 3D simulations with burnup-dependent pellet-clad friction, Nucl. Eng. Des. 242 (2012) 164–181.
[56] B. Baurens, J. Sercombe, C. Riglet-Martial, L. Desgranges, L. Trotignon, P. Maugis, 3D thermo-chemical-mechanical simulation of power ramps with ALCYONE fuel code, J. Nucl. Mater. 452 (1-3) (2014) 578–594.
[57] D. Pizzocri, F. Cappia, L. Luzzi, G. Pastore, V.V. Rondinella, P. Van Uffelen, A semi-empirical model for the formation and depletion of the high burnup structure in UO_2, J. Nucl. Mater. 487 (2017) 23–29.
[58] D. Pizzocri, T. Barani, L. Luzzi, SCIANTIX: a new open source multi-scale code for fission gas behaviour modelling designed for nuclear fuel performance codes, J. Nucl. Mater. 532 (2020) 152042.
[59] T.J. Gerczak, C.M. Parish, P.D. Edmondson, C.A. Baldwin, K.A. Terrani, Restructuring in high burnup UO_2 studied using modern electron microscopy, J. Nucl. Mater. 509 (2018) 245–259.
[60] M. Veshchunov, V. Shestak, Model for evolution of crystal defects in UO_2 under irradiation up to high burn-ups, J. Nucl. Mater. 384 (1) (2009) 12–18.
[61] M.S. Veshchunov, V.D. Ozrin, V.E. Shestak, V.I. Tarasov, R. Dubourg, G. Nicaise, Development of the mechanistic code MFPR for modelling fission-product release from irradiated UO_2 fuel, Nucl. Eng. Des. 236 (2) (2006) 179–200.
[62] A. Kolmogorov, On the statistical theory of metal crystallization, Izv. Akad. Nauk SSSR, Ser. Math (1937) 335–360.
[63] M. Kinoshita, Mesoscopic approach to describe high burn-up fuel behaviour, in: Enlarged HPG Meeting on High Burn-Up Fuel Performance, Safety and Reliability and Degradation of In-Core Materials and Water Chemistry Effects and Man-Machine Systems Research, Loen (Norway), 24-29 May 1999, 1999.
[64] J. Noirot, Y. Pontillon, S. Yagnik, J.A. Turnbull, Post-irradiation examinations and high-temperature tests on undoped large-grain UO_2 discs, J. Nucl. Mater. 462 (2015) 77–84.
[65] D. Pizzocri, G. Pastore, T. Barani, A. Magni, L. Luzzi, P. Van Uffelen, S. Pitts, A. Alfonsi, J. Hales, A model describing intra-granular fission gas behaviour in oxide fuel for advanced engineering tools, J. Nucl. Mater. 502.
[66] J. Spino, J. Rest, W. Goll, C. Walker, Matrix swelling rate and cavity volume balance of UO_2 fuels at high burn-up, J. Nucl. Mater. 346 (2) (2005) 131–144.
[67] E. Ruzauskas, K. Fardell, Design, Operation, and Performance Data for High Burnup PWR Fuel from the H. B. Robinson Plant for Use in the NRC Experimental Program at Argonne National Laboratory, Tech. Rep. Electric Power Research Institute, Palo Alto, CA, US, 2001, p. 1001558.
[68] A. Schubert, P. Van Uffelen, J. van de Laar, C. Walker, W. Haeck, Extension of the TRANSURANUS burn-up model, J. Nucl. Mater. 376 (1) (2008) 1–10.
[69] J. Noirot, J. Lamontagne, N. Nakae, T. Kitagawa, Y. Kosaka, T. Tverberg, Heterogeneous UO_2 fuel irradiated up to a high burn-up: investigation of the HBS and of fission product releases, J. Nucl. Mater. 442 (1-3) (2013) 309–319.
[70] J.W. Cahn, Transformation kinetics during continuous cooling, Acta Metall. 4 (6) (1956) 572–575.
[71] J. Noirot, I. Zacharie-Aubrun, T. Blay, Focused ion beam–scanning electron microscope examination of high burn-up UO_2 in the center of a pellet, Nucl. Eng. Technol. 50 (2018) 259–267.
[72] A.H. Booth, A Method of Calculating Fission Gas Diffusion from UO_2 Fuel and its Application to the X-2-F Loop Test, Atomic Energy of Canada Limited Chalk River Project Research and Development, Report AECL-496, vol. 496, 1957, pp. 1–23.
[73] R.J. White, M.O. Tucker, A new fission-gas release model, J. Nucl. Mater. 118 (1) (1983) 1–38.
[74] M. Speight, A calculation on the migration of fission gas in material exhibiting precipitation and Re-solution of gas atoms under irradiation, Nucl. Sci. Eng. 37 (1969) 180–185.
[75] G. Pastore, D. Pizzocri, C. Rabiti, T. Barani, P. Van Uffelen, L. Luzzi, An effective numerical algorithm for intra-granular fission gas release during non-equilibrium trapping and resolution, J. Nucl. Mater. 509 (2018) 687–699.
[76] R.L. Williamson, J.D. Hales, S.R. Novascone, M.R. Tonks, D.R. Gaston, C.J. Permann, D. Andrs, R.C. Martineau, Multidimensional multiphysics simulation of nuclear fuel behavior, J. Nucl. Mater. 423 (1-3) (2012) 149–163.

[77] G. Pastore, L.P. Swiler, J.D. Hales, S.R. Novascone, D.M. Perez, B.W. Spencer, L. Luzzi, P. Van Uffelen, R.L. Williamson, Uncertainty and sensitivity analysis of fission gas behavior in engineering-scale fuel modeling, J. Nucl. Mater. 456 (2015) 398–408.
[78] H.J. Matzke, Xenon migration and trapping in doped ThO_2, J. Nucl. Mater. 21 (2) (1967) 190–198.
[79] R.W. Grimes, C.R.A. Catlow, The stability of fission products in uranium dioxide, Philos. Trans. R. Soc. London. Ser. A Phys. Eng. Sci. 335 (1639) (1991) 609–634.
[80] D.R. Olander, Fundamental Aspects of Nuclear Reactor Fuel Elements, 1976.
[81] H. Kleykamp, The chemical state of the fission products in oxide fuels, J. Nucl. Mater. 131 (2-3) (1985) 221–246.
[82] S.C. Middleburgh, R.W. Grimes, K.H. Desai, P.R. Blair, L. Hallstadius, K. Backman, P. Van Uffelen, Swelling due to fission products and additives dissolved within the uranium dioxide lattice, J. Nucl. Mater. 427 (1) (2012) 359–363.
[83] R. Ducher, R. Dubourg, M. Barrachin, A. Pasturel, First-principles study of defect behavior in irradiated uranium monocarbide, Phys. Rev. B 83 (2011) 104107.
[84] M. Klipfel, V. Di Marcello, A. Schubert, J. van de Laar, P. Van Uffelen, Towards a multiscale approach for assessing fission product behaviour in UN, J. Nucl. Mater. 442 (1) (2013) 253–261.
[85] F. Kremer, R. Dubourg, F. Cappia, V.V. Rondinella, A. Schubert, P. Van Uffelen, T. Wiss, High burn up structure formation and growth and fission product release modelling: new simulations in the mechanistic code MFPR-F, in: TopFuel 2018, Prague, Czech Republic, 2018.
[86] L. Thomas, Condensed-phase xenon and krypton in UO_2 spent fuel, in: S. Donnelly, J.H. Evans (Eds.), Fundamental Aspects of Inert Gases in Solids, Springer US, 1991, pp. 431–441.
[87] K. Nogita, K. Une, High resolution TEM observation and density estimation of Xe bubbles in high burnup UO_2 fuels, Nucl. Instrum. Methods Phys. Res. Sect. B Beam Interact. Mater. Atoms 141 (1998) 481–486.
[88] P. Losonen, On the behaviour of intragranular fission gas in UO_2 fuel, J. Nucl. Mater. 280 (1) (2000) 56–72.
[89] C. Ronchi, Extrapolated equation of state for rare gases at high temperatures and densities, J. Nucl. Mater. 96 (3) (1981) 314–328.
[90] M. Kinoshita, T. Sonoda, S. Kitajima, A. Sasahara, E. Kolstad, H. Matzke, V. Rondinella, A. Stalios, C. Walker, I. Ray, M. Sheindlin, D. Halton, C. Ronchi, High burnup rim project (II) irradiation and examination to investigate rim-structured fuel, in: ANS International Topical Meeting on Light Water Reactor Fuel Behavior, April 9-13, 2000, Park City, UT, US, 2000.
[91] J.A. Turnbull, R.J. White, C. Wise, The diffusion coefficient for fission gas atoms in uranium dioxide, in: International Working Group on Water Reactor Fuel Performance and Technology, Technical Committee on Water Reactor Fuel Element Computer Modelling in Steady State, Transient and Accident Conditions, Preston, U.K., 1989.
[92] S. Brémier, C. Walker, Radiation-enhanced diffusion and fission gas release from recrystallised grains in high burn-up UO_2 nuclear fuel, Radiat. Eff. Defect Solid 157 (3) (2002) 311–322.
[93] F.S. Ham, Theory of diffusion-limited precipitation, J. Phys. Chem. Solid. 6 (4) (1958) 335–351.
[94] J.A. Turnbull, The distribution of intragranular fission gas bubbles in UO_2 during irradiation, J. Nucl. Mater. 38 (1971) 203–212.